Linear colloidal crystal arrays by electrohydrodynamic printing

H. F. Poon, D. A. Saville,[a] and I. A. Aksay[b]
Department of Chemical Engineering, Princeton University, Princeton, New Jersey 08544, USA

(Received 6 August 2008; accepted 8 September 2008; published online 2 October 2008)

We use electrohydrodynamic jets of colloidal suspensions to produce arrays of colloidal crystalline stripes on surfaces. A critical factor in maintaining a stable jet is the distance of separation between the nozzle and the surface. Colloidal crystalline stripes are produced as two wetting lines of the deployed suspension merge during drying. To ensure that the two wetting lines merge, the "deployed-line-width" to "particle size" ratio is kept below a critical value so that the capillary forces overcome the frictional forces between the particles and the substrate. © *2008 American Institute of Physics*. [DOI: 10.1063/1.2990680]

One- and two-dimensional (2D) colloidal structures are important building blocks and have been widely used for higher order architectures—nanowires,[1,2] photonic bandgap microstrips,[3] electronic and optical devices,[4–6] microchip reactors,[7] and biosensors.[8] Methods used for the aggregation of colloidal particles into ordered patterns have utilized masks,[9] stamps,[10] or prepatterned surfaces.[11] Since these methods require an extra step in the preparation of either a mask or a prepatterned surface, we utilize an electrohydrodynamic printing (EHDP) technique that eliminates the need for prior surface preparation.

In EHDP, we employ the cone-jet transition[12] to provide a large "neck-down" ratio ($\sim 10^2$ to 10^3) between the nozzle orifice and the jet diameter [Fig. 1(a)], which eliminates one of the inherent limitations of the ink-jet technology in nozzle clogging as millimeter size nozzles can now be used to produce micron diameter jets. Cone-jet transition takes place as the electrical stress arising from the surface charges on a pendent drop counteracts the surface tension force and deforms the drop into a Taylor cone[12] with a thin jet emanating from the conical tip. Thus, a main challenge in utilizing cone-jet transition for printing applications is to suppress the varicose and whipping (i.e., axisymmetric and nonaxisymmetric) instabilities[13–18] for the steady deployment of the jet. The inability to suppress these instabilities has limited the cone-jet technology only for coating applications through electrospinning with a deployment accuracy of ± 1 mm.[16] In EHDP, we keep the jet intact and straight by using closely separated electrodes to prevent the further growth of disturbances.[19,20]

A second key challenge in EHDP is the prevention of capillary breakup of the deployed jets on the substrate so that continuous lines can be printed. Suspension lines on the surface are subject to a 2D version of Rayleigh instability,[21,22] which causes them to break up into islands. The degree of wetting plays a crucial role on the breakup rate. For instance, the breakup is slower with wetting fluids than nonwetting fluids in the absence of contact line pinning. With wetting fluids, instability is completely suppressed if the contact lines are pinned on a substrate,[22] which is the case for the work described in this paper.

An EHDP instrument, as schematically illustrated in Fig. 1(a), was developed to demonstrate the principal of colloidal crystal patterning on surfaces. A nozzle with a relatively large orifice (stainless steel needle with an outer diameter 580 μm and inner diameter 370 μm) was used to avoid clogging. A dc electric field ($\sim 5\times 10^5$ V/m across the nozzle and the substrate) was applied (Model 620A, Trek Inc., Beaverton, OR) to induce the cone-jet transition.[12] The colloidal jets thus formed were then steadily deployed on a substrate to "write" colloidal patterns. Parallel colloidal lines were produced by placing a silicate glass substrate on top of a metal disk attached to a rotary motor (M 3353 motor, Baldor Electric Co., Fort Smith, AR) with a frequency controller (Model FR-U11OW-0.1K-UL, Mitsubishi Electric Corp., Japan), while the nozzle moving in the radial direction [Fig. 1(a)]. Colloidal suspensions in de-ionized water and ethanol solutions [~9.5 vol % 2 μm polystyrene (PS) particles from Duke Scientific and 0.01 g/ml of polyethylene oxide (PEO) with a molecular weight of 4×10^6 g/mol] were fed from a syringe to the nozzle through a Teflon tubing, with the flow rate controlled by a syringe pump (Model: Harvard 33 Twin Syringe Pump, Harvard Apparatus, Holliston, MA).

To obtain a stable jet, we (i) decreased the surface charge density of the jet, (ii) increased the suspension viscosity, and

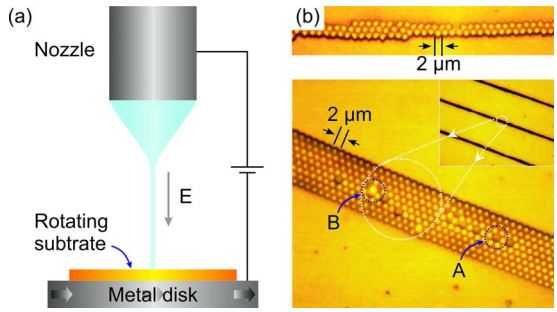

FIG. 1. (Color online) (a) The schematic diagram of EHDP apparatus for the deployment of a suspension jet. The nozzle is grounded and a negative high voltage is applied between nozzle and the disk. (b) Almost perfect crystalline linear arrays of PS latex (2 μm diameter) produced by EHDP on a silicate glass substrate. Patterns were imaged with a CCD camera mounted on a Leitz Metallovert optical microscope. The bottom image depicts a typical section of a one-dimensional colloidal crystal. A and B indicate the positions of a point defect and the presence of an additional particle on top of the array, respectively. The inset (~1200 μm wide) shows the overall appearance of the colloidal line pattern. The top image illustrates a continuous two-particle-wide array with three-particle defect.

[a]Deceased.
[b]Electronic mail: iaksay@princeton.edu.

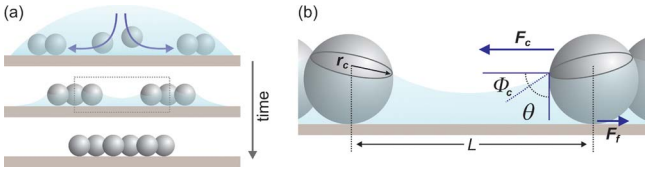

FIG. 2. (Color online) (a) Schematic illustration of the colloidal crystal formation during the drying process of a deployed suspension line. Two stripes of colloidal aggregates form at the edges of the lines due to evaporative convective flow. Below a critical linewidth of deployed pattern, two stripes of aggregates merge to yield a single stripe of colloidal crystal as (b) the capillary force F_c exceeds the frictional force F_f.

(iii) most importantly, decreased the separation distance (<1 mm) between the nozzle and the substrate. Since the conductivity of the electrosterically or electrostatically stabilized colloidal suspensions is high[23] (e.g., PS latex suspension as received in our experiments was $\sim 270\ \mu$S/cm, cf. $\sim 1\ \mu$S/cm for de-ionized water), the surface charge density of the jets was also intrinsically high; thus, the charge density had to be reduced to minimize the instabilities of the jets. Even after decreasing the conductivity of the suspensions by replacing 50% of water in the suspension with ethanol, however, the stabilization of the jets was not always achieved.[19]

Increasing the viscosity of the suspensions by adding PEO to the solutions had the effect of decreasing the growth rate of disturbances[13] and suppressing the rebound or splashing during the jet impact process.[24] The PEO concentration (~ 0.01 g/ml) of the solutions used in our experiments was greater than the overlap concentration, 1.5×10^{-3} g/ml in water, estimated from extrapolation of the literature data.[25] The addition of ~ 0.01 g/ml of PEO to the suspension increased the viscosity by approximately 1800%, and this was more than enough to eliminate the splashing.[24]

By keeping the separation between the nozzle and the substrate below 1 mm, our intent was not to allow sufficient time for the growth of whipping instability. However, more importantly than our original intention, a most beneficial aspect of this short separation distance is that when the radial electric field is higher than the ionization threshold of the surrounding gas, the short working distance enhances gas ionization and leads to partial discharging of the surface charge.[26] A useful consequence of the reduction in the surface charge of the jets is the suppression of the growth rates of whipping disturbances.

Colloidal assembly within the deployed lines involves the evaporation-induced self-assembly of particles[27] with simultaneous receding of the contact fronts from both sides of the printed line (Fig. 2). As these two fronts merge, colloidal crystals form as a single line. The images in Fig. 1(b) demonstrate two characteristics of these colloidal crystal lines. The patterns are "clean" with no smattering of small clusters or particles in the "empty" regions (space between two printed lines). Further, the colloidal crystalline arrays are relatively defect-free [$\sim 2\%$ to 3% point defect (as vacancy or extra particle) density]. The defect density is significantly lower than the polycrystalline colloidal patterns formed by the field induced assembly[9] or the commonly observed "double stripe pattern" formed by evaporative drying.[28] Although we have not yet utilized an x-y table, the indications with our present setup are that the accuracy and the reproducibility of the printed lines are affected more by the homogeneity of the substrate than the accuracy of the motion system or the stability of the jet. As shown below, the homogeneity of the substrate affects the pinning of the liquid during the self-assembly of the particles and thus introducing variations on the structure of the printed lines.

Convective self-assembly of colloidal particles at a single contact line is well documented[6,29] and has been exploited in the fabrication of single-crystalline colloidal crystals.[6,27] However, when two contact lines are involved, colloidal crystals form independently at each contact line, leaving a large open space in between similar to what is observed in ink-jet printing applications[28] and the coffee stain formation.[29] Our results exemplified in Fig. 1 suggest that a pair of contact fronts moves (Fig. 2) and merges the colloidal clusters together to form a compact single crystalline array. Such cluster migration is accelerated by the capillary attraction between partially immersed particles.[30] During the drying process, colloidal particles consolidate at the contact fronts on both sides of the line by convective self-assembly [Fig. 2(a)].[29] Then, as the evaporation of the solvent continues, linewidth shrinks and particles become partially exposed [Fig. 2(b)]. The capillary attraction between the two nearest partially immersed particles (one from each cluster) arises from the deformation of the liquid meniscus and the asymmetric contact lines around the particle surface.[31] This force "drags" the two clusters toward each other with particles within the clusters bound to each other by the capillary pressure similar to that in a latex film.[32] Using the schematic of Fig. 2, we model the capillary attraction as[31] $F_c=(2\pi\gamma r_c^2 \sin^2\phi_c)/L$ at a separation distance $r_c \ll L \ll (\gamma/\Delta\rho g)^{\frac{1}{2}}$ and the total frictional force as[33] $F_f \sim n\mu_f F_z$ with F_z being the normal force exerted by a particle on the substrate: $F_z=2\pi\gamma r_c \sin\phi_c$.[31] Here, L is the nearest center-to-center distance between two partially immersed particles, one from each cluster, r_c is the radius of contact line on the particle surface, ϕ_c is the mean meniscus slope angle, θ is the contact angle of the liquid on the surface of the particle, $\Delta\rho$ is the density difference between the liquid and the air, g is the gravitational acceleration, n is the number of rows of particles in a cluster, accounting for the cluster size, and μ_f is the frictional coefficient between the PS particles and the glass under lubrication, defined as the ratio between the frictional force and the normal force to a surface. A balance between the total frictional force and the capillary attraction leads to a critical "linewidth" to "particle size" ratio, $L_c/r \sim (\sin\phi_c)/n\mu_f$, which determines the morphology of a colloidal line on evaporative drying. When $L_c/r \leq (\sin\phi_c)/n\mu_f$, the capillary attraction overcomes the friction force and brings the clusters together to form a compact array. This usually occurs when particles are initially confined in small widths, which is an advantage of EHDP. At large linewidths, the double-stripe pattern in a printed line[28] and the ring of a coffee stain[29] are observed.

We verified the existence of a critical linewidth to particle size ratio empirically by adjusting the initial width (L_o) of a colloidal line (Fig. 3). At a critical initial width of $\sim 80\ \mu$m, the line changes its morphology from a double-stripe pattern to a compact array [Fig. 3(b). Figure 3(b) clearly indicates the accelerated cluster migration when the capillary attraction sets in at small separations ($L<22\ \mu$m, $L_o<80\ \mu$m). A close-packed array is thus formed. For large initial widths ($L_o>80\ \mu$m), the double-stripe patterns are

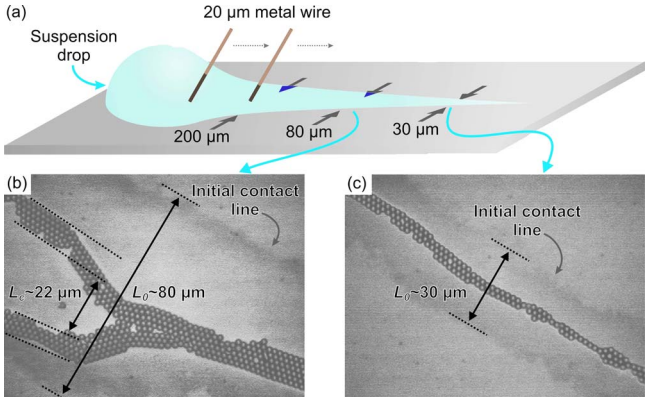

FIG. 3. (Color online) (a) The schematic of a colloidal dispersion line on a glass substrate with variable widths drawn from a colloidal drop of 3 mm diameter (drop not to scale) with a metal wire. [(b) and (c)] Optical microscope images of dried colloidal lines showing the transition from a double-stripe pattern to a single stripe as the initial width of deployed suspension line (L_o) decreases from 200 to 30 μm. L_p and L_c are the critical initial width for the transition and the corresponding nearest separation distance between two clusters. The initial contact line position is indicated by the dark stains formed from the deposition of solute upon evaporation. Panel (c) shows a dried solid line formed at small linewidths.

observed as the frictional force dominates and pinning occurs. The estimated μ_f from Fig. 3(b) is $\mu_f = (2\pi\gamma r_c^2 \sin^2 \phi_c)/(nL_cF_z) = (r_c \sin \phi_c)/(nL_c) \sim 0.008$ with $n \sim 5$, $L_c \sim 20r$, $r_c \sim r$, and $\phi_c = 50°$, where r is the particle radius. This is exactly the same order of magnitude as the reported values ($0.001 \sim 0.005$) of μ_f for lubricated polystyrene surfaces,[34] which further supports the phenomenon driven by a balance between the capillary attraction and the friction.

The electrohydrodynamic jet printing technique we report here combines the high resolution of an intact jet with contact-line-driven colloidal crystallization to rapidly print colloidal crystals over large areas. Both the axisymmetric and nonaxisymmetric instabilities in the colloidal jet are suppressed through a combination of reduced charge density on the jet and a closer proximity of the nozzle to the printing surface. As lines below a critical width are deployed, nearly perfect colloidal crystalline arrays form as the two wetting lines of the deployed suspensions merge during drying. For the system investigated in this study, this critical linewidth was ~80 μm. Although we used micron-sized particles to demonstrate the close-packed structure, the approach is potentially applicable to smaller particles, as the capillary interaction has been demonstrated significantly even with the colloidal assembly of nanometer-sized particles.[35,36]

Financial support for this work was provided by ARO-MURI under Award No. W911NF-04-1-0170 and the NASA University Research, Engineering and Technology Institute on Bio Inspired Materials (BIMat, Grant No. NCC-1-02037).

We acknowledge discussions with S. Korkut and her assistance in the preparation of the manuscript.

[1] A. K. Boal, F. Ilhan, J. E. DeRouchey, T. Thurn-Albrecht, T. P. Russell, and V. M. Rotello, Nature (London) **404**, 746 (2000).
[2] M. Li, H. Schnablegger, and S. Mann, Nature (London) **402**, 393 (1999).
[3] F. Falcone, T. Lopetegi, and M. Sorolla, Microwave Opt. Technol. Lett. **22**, 411 (1999).
[4] C. Haginoya, M. Ishibashi, and K. Koike, Appl. Phys. Lett. **71**, 2934 (1997).
[5] J. Boneberg, F. Burmeister, C. Schafle, P. Leiderer, D. Reim, A. Fery, and S. Herminghaus, Langmuir **13**, 7080 (1997).
[6] Y. A. Vlasov, X. Z. Bo, J. C. Sturm, and D. J. Norris, Nature (London) **414**, 289 (2001).
[7] H. Gau, S. Herminghaus, P. Lenz, and R. Lipowsky, Science **283**, 46 (1999).
[8] J. H. Holtz and S. A. Asher, Nature (London) **389**, 829 (1997).
[9] R. C. Hayward, D. A. Saville, and I. A. Aksay, Nature (London) **404**, 56 (2000).
[10] Y. D. Yin, Y. Lu, and Y. N. Xia, J. Mater. Chem. **11**, 987 (2001).
[11] Y. J. Sun and G. C. Walker, J. Phys. Chem. B **106**, 2217 (2002).
[12] A. M. Ganan Calvo, Phys. Rev. Lett. **79**, 217 (1997).
[13] D. A. Saville, Phys. Fluids **14**, 1095 (1971).
[14] M. M. Hohman, M. Shin, G. Rutledge, and M. P. Brenner, Phys. Fluids **13**, 2201 (2001).
[15] D. H. Reneker, A. L. Yarin, H. Fong, and S. Koombhongse, J. Appl. Phys. **87**, 4531 (2000).
[16] J. M. Deitzel, J. D. Kleinmeyer, J. K. Hirvonen, and N. C. B. Tan, Polymer **42**, 8163 (2001).
[17] I. Hayati, A. I. Bailey, and T. F. Tadros, J. Colloid Interface Sci. **117**, 205 (1987).
[18] J. F. de la Mora and I. G. Loscertales, J. Fluid Mech. **260**, 155 (1994).
[19] H. F. Poon, "Electrohydrodynamic printing," Ph.D. thesis, Princeton University, 2002.
[20] D. A. Czaplewski, J. Kameoka, R. Mathers, G. W. Coates, and H. G. Craighead, Appl. Phys. Lett. **83**, 4836 (2003).
[21] M. S. McCallum, P. W. Voorhees, M. J. Miksis, H. S. Davis, and H. Wong, J. Appl. Phys. **79**, 7604 (1996).
[22] S. Schiaffino and A. A. Sonin, J. Fluid Mech. **343**, 95 (1997).
[23] W. B. Russel, D. A. Saville, and W. R. Schowalter, *Colloidal Dispersions* (Cambridge University Press, Cambridge, England, 1989), pp. 258–327.
[24] V. Bergeron, D. Bonn, J. Y. Martin, and L. Vovelle, Nature (London) **405**, 772 (2000).
[25] K. Yuko and H. Chikako, Polym. Commun. **25**, 154 (1984).
[26] S. Korkut, D. A. Saville, and I. A. Aksay, Phys. Rev. Lett. **100**, 034503 (2008).
[27] J. F. Bertone, P. Jiang, K. S. Hwang, D. M. Mittleman, and V. L. Colvin, Phys. Rev. Lett. **83**, 300 (1999).
[28] T. Cuk, S. M. Troian, C. M. Hong, and S. Wagner, Appl. Phys. Lett. **77**, 2063 (2000).
[29] R. D. Deegan, O. Bakajin, T. F. Dupont, G. Huber, S. R. Nagel, and T. A. Witten, Nature (London) **389**, 827 (1997).
[30] N. D. Denkov, O. D. Velev, P. A. Kralchevsky, I. B. Ivanov, H. Yoshimura, and K. Nagayama, Langmuir **8**, 3183 (1992).
[31] P. A. Kralchevsky, V. N. Paunov, N. D. Denkov, I. B. Ivanov, and K. Nagayama, J. Colloid Interface Sci. **155**, 420 (1993).
[32] A. F. Routh and W. B. Russel, Langmuir **15**, 7762 (1999).
[33] A. W. Adamson and A. P. Gast, *Physical Chemistry of Surfaces*, 6th ed. (Wiley, New York, 1997), Chap. XII.
[34] J. Klein, E. Kumacheva, D. Mahalu, D. Perahia, and L. J. Fetters, Nature (London) **370**, 634 (1994).
[35] P. A. Kralchevsky and K. Nagayama, Langmuir **10**, 23 (1994).
[36] A. Böker, J. He, T. Emrick, and T. P. Russell, Soft Matter **3**, 1231 (2007).